Fieldwide Determination of Directional Permeabilities Using Transient Well Testing

Yan Pan, Medhat M. Kamal, and **Wayne Narr,** Chevron

Summary

We present here a practical method for estimating the directional permeabilities in anisotropic reservoirs. The method uses pressure transient-analysis results from at least three sets of interference/pulse tests among wells offset at different azimuths. Knowledge of the maximum/minimum permeability directions in anisotropic reservoirs helps to optimize injector/producer locations and is important for reservoir management, especially under secondary/enhanced recovery of hydrocarbons. The proposed method uses transient-test data rich with dynamic information to provide fieldwide permeability distribution at well-spacing scale, which is relevant for estimating fluid movement and recovery. Its application in a carbonate oil field in Kazakhstan is also discussed.

The proposed method uses well coordinates and multiple sets of analysis results of interwell transient tests through mathematical matrix operations. It is straightforward to use and works efficiently. The algorithms to calculate directional permeabilities in anisotropic homogeneous reservoirs from interference tests were first introduced by Ramey (1975) and extended to pulse tests by Kamal (1983). Our new approach can use the analysis results of any type of interwell transient test directly in heterogeneous reservoirs. Any valid modern methods can be used to analyze each interwell test, and all analysis results can be integrated to generate the field permeability-tensor map.

The proposed method was validated using synthetic cases. Its application in a large set of multiple-well tests in a naturally fractured reservoir illustrated its practicality and efficiency. Extensive interwell transient data have been collected and analyzed from carefully designed and conducted tests among 12 wells in Korolev Field, a carbonate field in Kazakhstan. Of the 12 wells, 10 have interwell tests at three different directions, which allows the calculation of directional permeabilities. The permeability-tensor map is generated for the entire field and compared with the fracture orientations derived from geological-structure and image-log interpretation. Both static and dynamic data resources indicate that fracture orientations vary substantially throughout the field. In some areas, the dominant permeability directions from interwell transient data are consistent with those from image-log interpretation. However, they differ in other areas, emphasizing the need for using dynamic measurements at well-spacing scale for better understanding of fracture distributions/orientations and their effects on flow communication among wells.

The novelty of this method of estimating directional permeabilities is that it uses well coordinates and analysis results of individual interwell transient tests directly in heterogeneous reservoirs. It is convenient and efficient. It can be easily used to generate a fieldwide permeability-tensor map using dynamic transient data. Its application in a large carbonate reservoir demonstrates its practicality, even in fields with complex varying anisotropy. Integrating the results from this method with those from geological and petrophysical analyses reduces uncertainty in reservoir characterization. This method has already been implemented in some commercial well-test-analysis software.

Introduction

The knowledge of flow communication between wells is key information for reservoir management, especially in secondary or tertiary recovery. The surveillance methods to collect dynamic data to gain such knowledge include multiple-well pressure transient tests (PTTs) and tracer tests. The measurements of tracer agents arriving at producing wells provide direct confirmation of flow communication. Interwell transient tests derive similar information through the measurements of pressure responses at observation wells to the production- or injection-rate changes at an active well, and the time required to conduct such a test is much shorter than that for a tracer test. For anisotropic reservoirs, such as naturally fractured fields or a channel system, knowing the permeability-tensor directions and the ratios of maximum/minimum permeability in various locations in the field provides a better chance to make optimal operation decisions.

The analytical solution for pressure responses at any location to a line-source well in an anisotropic system was first presented by Papadopulos (1965). Ramey (1975) introduced the method to analyze interference tests in anisotropic oil/gas reservoirs to calculate the directional permeabilities. Kamal and Brigham (1976) proposed the procedures for designing and analyzing pulse tests with unequal pulse and shut-in periods, and Kamal (1983) further extended the methods to estimate dominant permeabilities in anisotropic reservoirs. All methods require three sets of interference or pulse tests among wells offset at different azimuths, and the pressure-response data are analyzed simultaneously using pressure and time matching data with type curves to calculate permeability tensors.

In practice, there is a limited chance to conduct all three sets of interference tests through the same well at one time and analyze them simultaneously to derive the permeability tensor. Interwell tests are conducted either by planning or as the operation opportunity arises for various project objectives, and are usually analyzed one set at a time. As field development progresses, more and more interference data are collected in the field, and at a certain stage there might be enough data to calculate directional permeability at different locations. In this paper, we propose a new practical method to use previous test-analysis results directly to estimate the permeability tensor, without the need to locate the exact matching-point pressure and time for each test. This method has already been implemented in some commercial well-test-analysis software. The analysis results (the permeability and porosity of the fast path linking two wells) from a single-set interwell (interference or pulse) test could be obtained using any modern techniques, such as analytical, semianalytical, or numerical models, and is not limited to conventional-type-curve matching. The algorithm uses mathematical matrix operations, and all analysis results can be integrated to generate the field permeability-tensor map.

This paper (SPE 181437) was accepted for presentation at the SPE Annual Technical Conference and Exhibition, Dubai, 26–28 September 2016, and revised for publication. Original manuscript received for review 25 May 2017. Revised manuscript received for review 27 May 2018. Paper peer approved 6 June 2018.

Method

For any interference test between two wells, by analyzing the pressure response at the observation well and the rate change at the active well, the permeability and porosity of the fast path linking the two wells can be estimated from Eqs. 1a and 1b at the matching points of data and a homogeneous isotropic model.

$$p_D = \frac{h \cdot (p_i - p_{x,y,t})}{141.2 \cdot qB\mu} \cdot k, \quad \ldots\ldots (1a)$$

$$\frac{t_D}{r_D^2} = \left(\frac{0.000264 \cdot t}{\mu \cdot c_t}\right) \cdot \left(\frac{k}{\phi \cdot r^2}\right). \quad \ldots\ldots (1b)$$

For an anisotropic homogeneous reservoir, Ramey (1975) proposed using type-curve matching for three sets of interference tests conducted at different directions (**Fig. 1**) to derive the permeability tensor. The pressure matches (Eq. 2a) of the three sets will provide similar estimation of the effective permeability, $k^{\text{eff}} = \sqrt{k_{xx} \cdot k_{yy} - k_{xy}^2}$. The time matches (Eq. 2b) will add three more equations to solve for k_{xx}, k_{yy}, k_{xy}, and ϕ.

$$p_D = \frac{h \cdot (p_i - p_{x,y,t})}{141.2 \cdot qB\mu} \cdot \sqrt{k_{xx} \cdot k_{yy} - k_{xy}^2}, \quad \ldots\ldots (2a)$$

$$\frac{t_D}{r_D^2} = \left(\frac{0.000264t}{\phi\mu \cdot c_t}\right) \cdot \left(\frac{k_{xx} \cdot k_{yy} - k_{xy}^2}{k_{xx} \cdot y^2 + k_{yy} \cdot x^2 - 2k_{xy} \cdot xy}\right). \quad \ldots\ldots (2b)$$

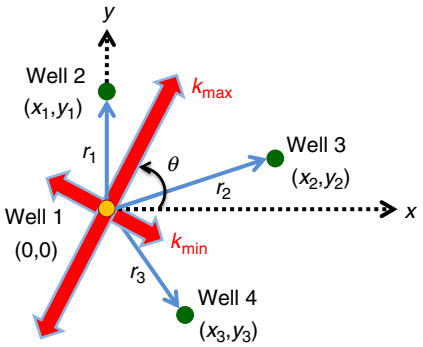

Fig. 1—Determining directional permeability from three sets of interwell tests.

Finally, using Eqs. 3a, 3b, and 3c, the maximum and minimum permeabilities and the angle θ relative to well-location coordinates, respectively, can be calculated.

$$k_{\max} = \frac{1}{2}\left[(k_{xx} + k_{yy}) + \sqrt{(k_{xx} - k_{yy})^2 + 4k_{xy}^2}\right], \quad \ldots\ldots (3a)$$

$$k_{\min} = \frac{1}{2}\left[(k_{xx} + k_{yy}) - \sqrt{(k_{xx} - k_{yy})^2 + 4k_{xy}^2}\right], \quad \ldots\ldots (3b)$$

$$\theta = \arctan\left(\frac{k_{\max} - k_{xx}}{k_{xy}}\right). \quad \ldots\ldots (3c)$$

The matching points ($p_{x,y}$, t) from each pair of the three interference tests are used to solve Eqs. 2a and 2b simultaneously to derive the permeability tensor.

For a pulse test, where the rate changes at an active well have a repeated pattern, Kamal (1983) provided the solution for an anisotropic reservoir (Eqs. 4a and 4b). After solving k_{xx}, k_{yy}, k_{xy}, and ϕ from three sets of pulse tests, the same Eqs. 3a, 3b, and 3c can be used to estimate directional permeabilities.

$$\Delta p_D = \frac{h \cdot \Delta p}{70.6qB\mu} \cdot \sqrt{k_{xx} \cdot k_{yy} - k_{xy}^2}, \quad \ldots\ldots (4a)$$

$$\Delta t_{cD} = \left(\frac{\Delta t_c}{948.333 \cdot \phi\mu \cdot c_t}\right) \cdot \left(\frac{k_{xx} \cdot k_{yy} - k_{xy}^2}{k_{xx} \cdot y^2 + k_{yy} \cdot x^2 - 2k_{xy} \cdot xy}\right). \quad \ldots\ldots (4b)$$

The pressure-response magnitude Δp and time lag Δt from each pair of the three pulse tests are used to solve Eqs. 4a and 4b simultaneously to derive the permeability tensor.

In this paper, we propose a new practical method to use previous analysis results of individual sets of interwell tests to directly estimate the permeability tensor instead of the measurement values of the matching data points, which might be difficult to locate among old tests. The analysis results could be obtained using any modern or conventional techniques. Then, the permeability tensor at the center well (Well 1 in Fig. 1) can be calculated from analysis-result sets of three interwell tests using Eqs. 5a and 5b.

$$\vec{k_i} = \begin{bmatrix} k_{xx} \\ k_{yy} \\ k_{xy} \end{bmatrix} = \frac{(k^{\text{eff}})^2}{\phi} \cdot \begin{bmatrix} dy_1^2 & dx_1^2 & -2dx_1 \cdot dy_1 \\ dy_2^2 & dx_2^2 & -2dx_2 \cdot dy_2 \\ dy_3^2 & dx_3^2 & -2dx_3 \cdot dy_3 \end{bmatrix}^{-1} \cdot \begin{bmatrix} r_1^2\phi_1/k_1 \\ r_2^2\phi_2/k_2 \\ r_3^2\phi_3/k_3 \end{bmatrix} = \frac{(k^{\text{eff}})^2}{\phi} \cdot [\boldsymbol{M}_{ij}]^{-1} \cdot \vec{\boldsymbol{R}}_j, \quad (5a)$$

$$k^{\text{eff}} = \sqrt{k_{xx} \cdot k_{yy} - k_{xy}^2}, \quad (5b)$$

where $(dx, dy)_i$ are the coordinates of wells relative to the center well, r_i is the well distance to the center well, and k_j and ϕ_j are individual interwell-test-analysis results. Thus, the permeability tensor $\boldsymbol{k}_i$ can be directly derived from the mathematical operations of the well-location matrix $\boldsymbol{M}_{ij}$ and the individual interwell analysis-result tensor $\boldsymbol{R}_j$.

Eqs. 5a and 5b can be further organized for matrix calculation. If we define the inverse matrix of $\boldsymbol{M}_{ij}$ as $\boldsymbol{N}_{ij} = (\boldsymbol{M}_{ij})^{-1}$, the following relation can be derived:

$$\phi = k^{\text{eff}} \cdot \sqrt{\left(\sum_j \boldsymbol{N}_{1j} \cdot R_j\right) \cdot \left(\sum_j \boldsymbol{N}_{2j} \cdot R_j\right) - \left(\sum_j \boldsymbol{N}_{3j} \cdot R_j\right)^2} = k^{\text{eff}} \cdot \alpha, \quad (6a)$$

$$\vec{k_i} = \frac{k^{\text{eff}}}{\alpha} \cdot [\boldsymbol{N}_{ij}] \cdot \vec{R}_j. \quad (6b)$$

The obtained k_{xx}, k_{yy}, k_{xy}, and ϕ are then used in Eqs. 3a through 3c to calculate $k_{\max}$, $k_{\min}$, and θ.

Validation

The method is tested on a synthetic case **(Fig. 2).** It is a homogeneous anisotropic oil reservoir with porosity of 0.05, dominant maximum permeability of 316 md in the x-direction, and minimum permeability 10 times smaller at 31.6 md in the y-direction. The effective permeability $k^{\text{eff}} = \sqrt{k_{xx} \cdot k_{yy} - k_{xy}^2}$ is 100 md. Three pulse tests are conducted among four wells. The center well is Well 1 as the pulsing well. One test is at the x-direction between Wells 1 and 2, another is at the y-direction between Wells 1 and 3, and another at a 60° angle between Wells 1 and 4. Wells 2, 3, and 4 are at the same distance ($r = 1000$ m) away from Well 1, the center well.

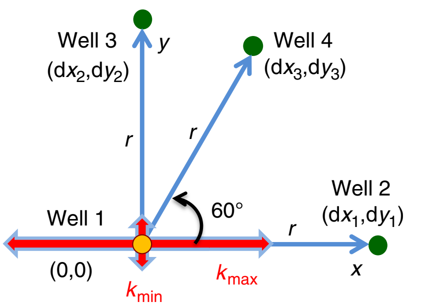

Fig. 2—Synthetic case of homogeneous anisotropic reservoir.

As shown in **Fig. 3,** by analyzing the individual-interwell-test data (green) using an isotropic homogeneous model (red), the permeability and porosity of the path linking each pair of wells are obtained **(Table 1).**

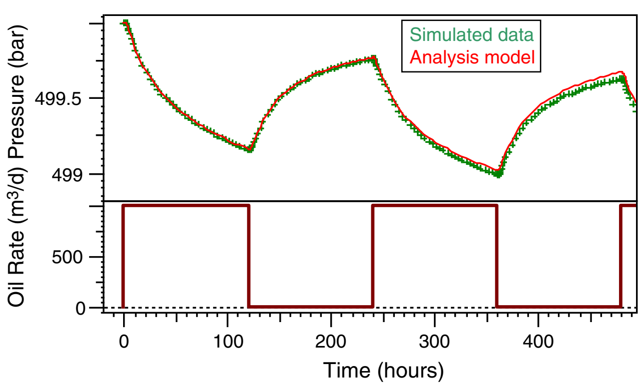

Fig. 3—Case 1: Transient analysis of pulse test between Wells 1 and 2.

The effective permeabilities estimated from three sets of tests are similar, between 93 and 97 md. The estimated effective permeability is derived from the pressure match and is a function of the effective permeability of the anisotropic homogeneous system (Eqs. 2a and 4a), no matter the direction of the interwell test. The estimated porosity in each direction is directly proportional to the time lag (Eqs. 2b and 4b). For the test between Wells 1 and 2 in the maximum permeability (x) direction, the time lag is the shortest and the derived porosity is the smallest. For the interwell test in the y-direction, the time lag is the longest and leads to the largest porosity

estimation among the tests in three directions. This is consistent with the observations by Ramey (1975) and Kamal (1983). These results are the first estimates assuming an isotropic homogeneous system. Results such as these that are obtained during analysis of field data, where we do not know a priori the type of system we have, are clear indications that we are dealing with an anisotropic system. We know porosity is a scaler quantity and permeability is a function of direction. However, the results show the same permeability in different directions and different porosity values depending on the direction (Kamal 1979). The derived porosity and permeability values at this step do not represent the anisotropic system.

Interwell Test	Porosity ϕ	Permeability k (md)
Wells 1 and 2	0.017	96.6
Wells 1 and 3	0.163	94.3
Wells 1 and 4	0.129	93.2

Table 1—Synthetic case: Analysis results of individual interwell tests.

In the next steps, the anisotropic homogeneous system properties k_{xx}, k_{yy}, k_{xy}, and ϕ are calculated by solving the matrix system (Eqs. 6a and 6b) using the first estimations from the preceding step.

The relative locations of all well pairs (in m) are

$$(\mathrm{d}x, \mathrm{d}y)_i = \begin{bmatrix} \mathrm{d}x_1 & \mathrm{d}y_1 \\ \mathrm{d}x_2 & \mathrm{d}y_2 \\ \mathrm{d}x_3 & \mathrm{d}y_3 \end{bmatrix} = \begin{bmatrix} 1000 & 0 \\ 0 & 1000 \\ 500 & 866 \end{bmatrix}.$$

The location matrix $\boldsymbol{M}_{ij}$ and its inverse matrix $\boldsymbol{N}_{ij}$ (in m^2) for this case are

$$\boldsymbol{M}_{ij} = \begin{bmatrix} \mathrm{d}y_1^2 & \mathrm{d}x_1^2 & -2\mathrm{d}x_1 \cdot \mathrm{d}y_1 \\ \mathrm{d}y_2^2 & \mathrm{d}x_2^2 & -2\mathrm{d}x_2 \cdot \mathrm{d}y_2 \\ \mathrm{d}y_3^2 & \mathrm{d}x_3^2 & -2\mathrm{d}x_3 \cdot \mathrm{d}y_3 \end{bmatrix} = \begin{bmatrix} 0 & 1.0\times10^6 & 0 \\ 1.0\times10^6 & 0 & 0 \\ 7.5\times10^5 & 2.5\times10^5 & -8.66\times10^5 \end{bmatrix},$$

$$\boldsymbol{N}_{ij} = \left[\boldsymbol{M}_{ij}\right]^{-1} = \begin{bmatrix} 0 & 1.0\times10^{-6} & 0 \\ 1.0\times10^{-6} & 0 & 0 \\ 2.89\times10^{-7} & 8.66\times10^{-7} & -1.15\times10^{-6} \end{bmatrix}.$$

The individual interwell analysis-result tensor $\boldsymbol{R}_j$ (in m^2/md) (Table 1) is

$$\vec{\boldsymbol{R}}_j = \begin{bmatrix} r_1^2\phi_1/k_1 \\ r_2^2\phi_2/k_2 \\ r_3^2\phi_3/k_3 \end{bmatrix} = \begin{bmatrix} 175.8 \\ 1727 \\ 1383 \end{bmatrix}.$$

Using Eq. 6a and the average of the permeabilities estimated from the three individual pulse tests (Table 1), the average-porosity estimation is 0.052. The permeability tensor can then be derived from Eq. 6b as $\boldsymbol{k}_j = (298, 301, 8.7)^T$ md. The final step is using Eqs. 3a, 3b, and 3c to calculate $k_{\max}$, $k_{\min}$, and θ, which are 298 md, 30.1 md, and –1.9°, respectively. The results are compared with the input of the synthetic case **(Table 2).** The directional permeabilities from the proposed method have 3 to 7% error compared with the true values, and the angle is less than 2° from the input value. The discrepancy comes from the approximation with the isotropic reservoir when analyzing the pulse test of an individual well pair. Once the anisotropic nature of the field is confirmed through the study of existing interwell-test data, such as with this method, a reservoir model with directional permeabilities can be used to fine tune the parameter estimations.

	Porosity ϕ	Effective Permeability k^{eff} (md)	Maximum Permeability $k_{\max} = k_{xx}$ (md)	Minimum Permeability $k_{\min} = k_{yy}$ (md)	Permeability Element k_{xy} (md)	Angle of $k_{\max}$ θ (degrees)
True input	0.050	100	316	31.6	0.0	0.0
Estimation	0.052	93–97	298	30.1	8.7	–1.9
Error	2 to 6%	3 to 7%	4 to 7%	3 to 6%	<10 md	<2°

Table 2—Synthetic case: Comparison of derived directional permeabilities.

Field Application

The proposed method is applied in the carbonate Korolev Oil Field, which is a satellite of the supergiant Tengiz Field on the northeast shore of the Caspian Sea in Kazakhstan. Both fields are Middle Devonian to Upper Carboniferous isolated-carbonate platforms. Fractures are common and significantly enhance the productivity of Korolev Field and the outer platform and slope area of Tengiz Field (Tankersley et al. 2010; Collins et al. 2013). The crude oil in Korolev Field is sour (approximately 15% hydrogen sulfide) at 47 °API and a bubblepoint pressure of 3,650 psia. The field has been producing under primary depletion since 2001 (Abdrakhmanova et al. 2014; Levchenko et al. 2017).

Field-Application Background. Development of the reservoir model in Korolev Field is dependent on seismic, static (well logs and core), and dynamic [productivity-index (PI), PTT, and pulse-test) data. Seismic facies regions were mapped using 3D data acquired in

2010. The seismic facies were calibrated to available core data and complemented with interpretation using a formation microimager (FMI) (Bachtel et al. 2014). Initial fracture characterization included determining fracture density, porosity, orientation, aperture, length, and height. Fracture density was estimated from FMI logs, photoelectric and caliper logs, bit drops, lost-circulation zones, Stoneley-wave data, and temperature and production logs. Only potentially effective fractures were used to determine fracture density and porosity curves.

Dynamic data integration (DDI) (Pan et al. 2016; Levchenko et al. 2017) was used to determine how the observed dynamic responses at wells are predicted using the fracture trends. The simulated dynamic response generated using the fracture model was compared with actual PI, PTT, and pulse-test results. The fracture model was then modified at the areas needing improvement, and the process was repeated until an acceptable match was reached. Calibrations using the PI, PTT, and pulse test were used sequentially. The output from PI calibration was the input for PTT calibration, and the output was used as input for pulse-test calibration. Additional iterations might be necessary for certain situations.

Because the PI of a well is a function of the flow capacity (kh) in the drainage area around the well and its skin value, it can be used as a proxy for fracture density and connectivity. PIs are also available for all wells, and together with production-log data were used to identify trends for various producing intervals. The next step in DDI is to qualitatively match the pressure transient data measured in a well by applying conceptual trends in the fracture model that was previously calibrated using PI information. Lessons learned from this step indicate first that local-grid refinements around wells are needed to capture transient behavior, especially at early times. This is the same as documented in the literature (Kamal et al. 2005). Second, just like in actual field practices, other wells do not need to be shut in during simulation to calculate one well's transient behavior. Third, a long production history before the buildup test might not be needed in numerical simulation; only the influential duration is necessary, as expected from pressure transient-analysis theory. The last step in DDI is to use interwell transient-test data. One of the variables obtained from multiple well tests (interference and pulse tests) is directional permeability (Kamal 1983). Details of how this is achieved is the main objective of this paper and is described in the next subsection.

Use of Pulse-Test Data. Because the operator is seeking potential improved-oil-recovery opportunities for additional oil recovery, Korolev Field is selected as the pilot field. To understand the flow communication among wells and fracture orientation in the field, extensive interwell transient data have been collected from carefully designed and conducted tests among the 12 wells in Korolev Field from 2003 to 2015. The arrows in **Fig. 4** indicate successful interference or pulse tests between wells. Each interwell-test pair is analyzed using dual-porosity models with techniques in the literature (Kamal and Brigham 1976; Deruyck et al. 1982; Araujo et al. 1998; Kamal 2009). The obtained diffusivity (k/ϕ) ranges from tens to tens of thousands of millidarcies, confirming the heterogeneous nature of the carbonate field.

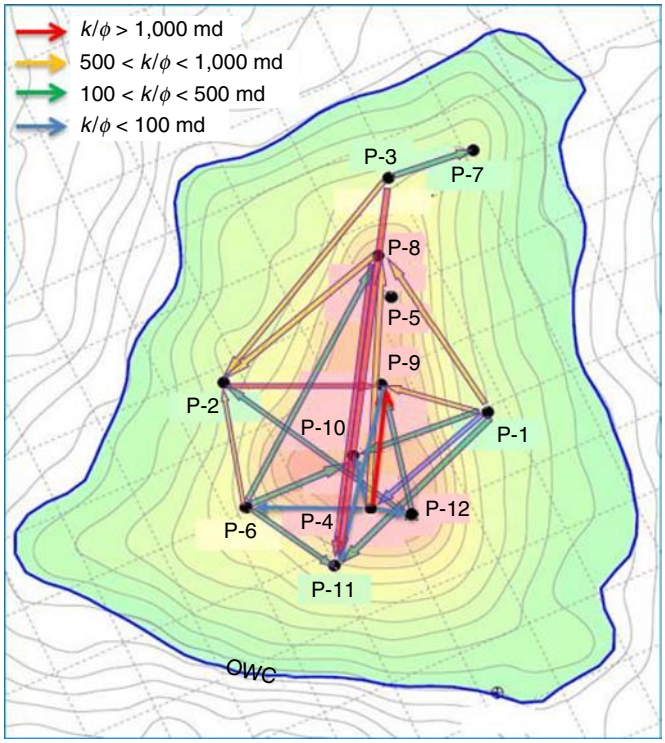

Fig. 4—Interwell tests in Korolev Field in Kazakhstan.

Fig. 5a shows the transient analysis of the pulse test between Wells P-6 and P-2 in the western area of Korolev Field. There were 4-day pulses of 1250-m^3/d rate change sent out from Well P-6, and the pressure at Well P-2 responded with a delay of 40 hours and an amplitude of approximately 0.01 bar. The pressure-derivative curve dp/dt clearly displays the correspondence. The 2006 buildup test at Well P-6 (Fig. 5b) and the 2003 buildup test at Well P-2 (Fig. 5c) show a distinguishable matrix/fracture interporosity-flow transient behavior (the trough on pressure-derivative curves in red). Therefore, a dual-porosity model is selected to match the pulse-test data in both the history plot and the log-log diagnosis plot of one pulse period (light blue), and the fast-path properties, permeability k, porosity ϕ, storativity ratio ω, and interporosity-flow coefficient λ, are estimated. As **Table 3** shows, the kh value obtained from the pulse test is five times larger than those from the individual buildup test at the wells, which is not uncommon in naturally fractured reservoirs. It

indicates that there is a conductive fracture network linking the two wells. The *kh* value from the single-well test is the effective average of the tested reservoir volume, including the fracture/matrix system near the well, whereas the pulse-test response is dominated by the most-conductive path (high k/ϕ value) linking the wells. If the *kh* values from the interwell and single-well tests are similar, this implies that the fracture distribution or the lack of it around the wells is the same as between the wells.

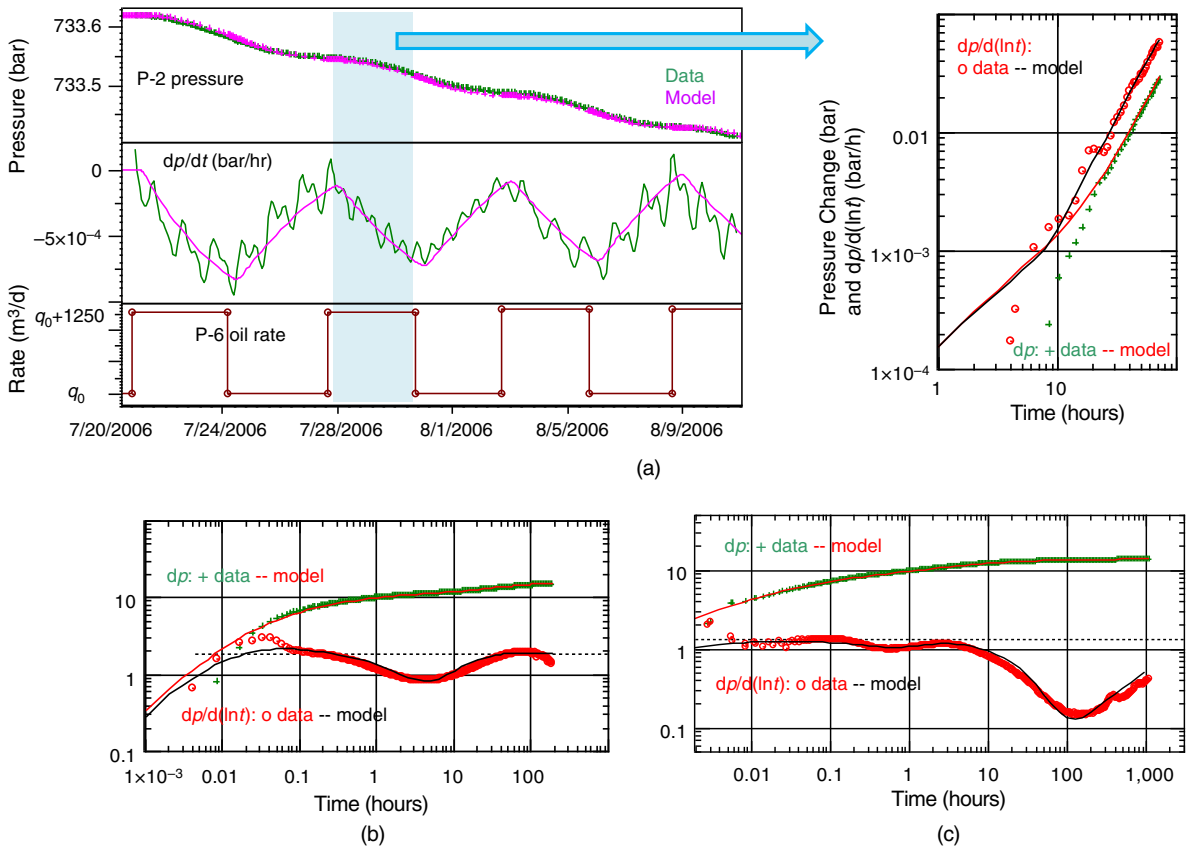

Fig. 5—(a) Transient analysis of interwell test between Wells P-6 and P-2 in Korolev Field. (b) The 2006 buildup test at Well P-6. (c) The 2003 buildup test at Well P-2.

Test Type	Well	Permeability × Net Pay *kh* (md·m)	Porosity × Net Pay ϕh (m)	Diffusivity k/ϕ(md)	Storativity Ratio ω	Interporosity-Flow Coefficient λ
Buildup	P-6	2200	37	59	0.18	1.8×10^{-6}
Buildup	P-2	1700	8	220	0.01	3.5×10^{-9}
Pulse test	P-6 and P-2	10 000	17	596	0.40	1.0×10^{-7}

Table 3—Properties from single-well and interwell tests between Wells P-6 and P-2.

An interference-test example in Korolev Field is shown in **Fig. 6.** In November 2008, there was an operational need to reduce production at Well P-3 in the north. Nearby Well P-7, with a permanent downhole gauge, collected the pressure responses to the rate change at Well P-3. It has an 85-hour time lag. The obtained fast-path properties are listed in **Table 4,** along with buildup-test results from these two wells. The flow communication between Wells P-3 and P-7 is confirmed. When analyzing the interference test with a dual-porosity model, the log-log plot of the pulse period is more sensitive to parameters ω and λ than the history plot is, and can be used to fine tune their values. Comparing the results, the fast-path matrix/fracture-system properties ω and λ tend to be bigger than the effective average values obtained from single-well buildup tests.

All interwell tests in Korolev Field (Fig. 4) are analyzed following the same procedure and using the single-well buildup-test results as references to seek clues regarding fracture distribution. Of the 12 interwell tests, 10 of them conducted in at least three directions. Well P-7 in the northeast of the field has only one interference test conducted, and Well P-5 in the north of the platform has no valid interwell-test data, so no directional permeability can be estimated. The permeability tensors at those 10 well locations are calculated using the proposed method (Eqs. 5a and 5b) from previous interference- or pulse-test-analysis results, and the maximum and minimum permeabilities and their directions are derived from the permeability tensors (Eqs. 3a, 3b, and 3c) **(Table 5).** Then a field map **(Fig. 7)** is generated showing the directional permeabilities in purple arrows. The sizes of the k_{max} and k_{min} arrows on the map are in a consistent scale relative to the derived values.

From geological information and static data, the dominant fracture trend and the orientations of effective fractures at each well location are also mapped (blue dashed curves in Fig. 7). Rose diagrams show the strike of effective fractures, which were measured with a borehole-image log. Effective fractures are interpreted to be those with the potential to affect flow to a well or within a reservoir (Narr et al. 2006). Fractures incorporated in the rose diagrams were identified on FMI borehole-image logs and interpreted for their likelihood

of flowing fluids, primarily depending on a production-logging-tool (PLT) flowmeter, flowing temperature, or lost-circulation data **(Fig. 8).** Most Korolev Field wells were drilled with oil-based mud, and therefore open fractures are electrically resistive because of the resistive mudcake or crude oil in the open-fracture aperture, as evident in Fig. 8. The dark fractures are probably filled with clay or other conductive mineralization, and are hence not effective.

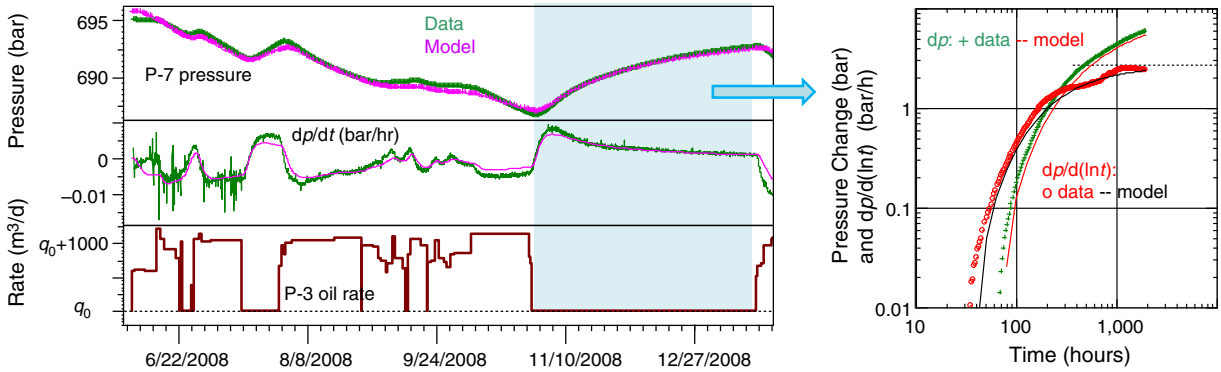

Fig. 6—Transient analysis of interwell test between Wells P-3 and P-7 in Korolev Field.

Test Type	Well	Permeability × Net Pay kh (md·m)	Porosity × Net Pay ϕh (m)	Diffusivity k/ϕ(md)	Storativity Ratio ω	Interporosity-Flow Coefficient λ
Buildup	P-3	300	37	153	0.06	5.5×10^{-9}
Buildup	P-7	40	14	3	0.01	2.0×10^{-5}
Pulse test	P-3 and P-7	856	4	207	0.10	3.0×10^{-6}

Table 4—Properties from single-well and interwell tests between Wells P-3 and P-7.

	P-1	P-2	P-3	P-4	P-6	P-8	P-9	P-10	P-11	P-12
k_{max} (md)	19.1	42.5	33.4	11.3	43.5	15.0	43.7	33.2	12.0	27.3
k_{min} (md)	3.5	8.5	2.5	9.8	8.3	4.4	4.4	6.8	2.0	1.6
θ (degrees)	12	64	69	80	85	78	32	27	81	–71

Table 5—Directional permeabilities at 10 well locations in Korolev Field.

From their visual character, the fractures include small-aperture cracks (red in Fig. 7; example shown at 4058 m in Fig. 8), solution-enlarged fractures (pink), and caverns/vugs (brown), which are an extreme development of solution enlargement. The effective fracture in Fig. 8 dips steeply to the south, and hence its strike would align with the east/west trend in the rose diagram of Well P-10 in Fig. 7. The rose-diagram scale in Fig. 7 is independent from that of the directional-permeability arrows from transient tests. The dominant trend of the fractures (blue dashed curve in Fig. 7) is dependent on our interpretive model of fractures parallel and perpendicular to the strike of the depositional margin of this carbonate buildup (Collins et al. 2013).

In most areas of the field, the maximum and minimum permeability directions from interwell transient data are consistent with those from static data. Fracture orientations vary substantially throughout the field, suggesting high variability in fracture-system character. For the four wells close to the rim (Wells P-2, P-6, P-11, and P-1), the derived maximum and minimum permeability directions (purple arrows in Fig. 7) align with the two sets of perpendicular fracture orientations (blue dashed curves) derived from the geological model, and the ratio of maximum to minimum permeability is more than five (Table 5). Depending on how the fractures were formed along the rim during carbonate buildup, the maximum permeability direction could be parallel to the rim orientation (Wells P-2 and P-6) but could also be perpendicular to the rim (Wells P-11 and P-1). Well P-3 in the north slope also shows strong anisotropy, but the directional permeabilities are slightly different from the fracture orientations in the geological model.

For the five wells on the platform where the fracture orientation is difficult to predict, three wells (Wells P-9, P-10, and P-12) show strong anisotropic ratios, whereas the other two (Wells P-4 and P-8) are close to isotropic. Compared with the rose diagram from the image logs, permeability tensors from interference transient data have relatively consistent directions at Wells P-8 and P-10, but differ at Wells P-9 and P-12. Considering that these two types of data sources have a notable difference in scale (image logs in inches and interference tests with well spacing in thousands of meters), it is not uncommon that the respective interpretation results are different. In addition, the transient tests provide dynamic flowing measurements between wells, whereas the image logs rely on the PLT to indicate which fractures crossing the wellbore are effective.

These permeability tensors obtained from dynamic data in the well-spacing scale help to understand fracture distributions, orientations, and their effects on flow communications among various wells in Korolev Field, and are key information for making reservoir-development plans. During primary recovery, the knowledge of permeability tensors could help to optimize the infill-drilling well spacing, which is smaller in the minor-permeability direction and larger in the dominant direction. For the secondary and tertiary recovery, this is especially important in choosing the locations of water or gas injectors to prevent early breakthrough and increase sweep efficiency. Currently, all the information from transient data and numerical full-field simulation studies is used to plan a large-scale waterflooding pilot in Korolev Field.

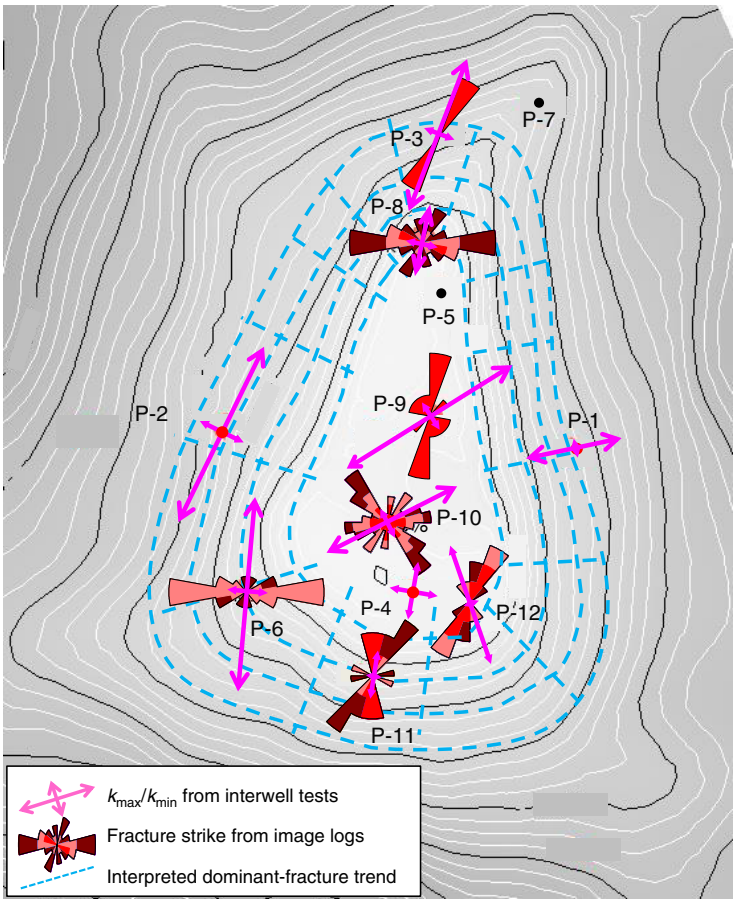

Fig. 7—Korolev Field fracture trend and directional permeabilities.

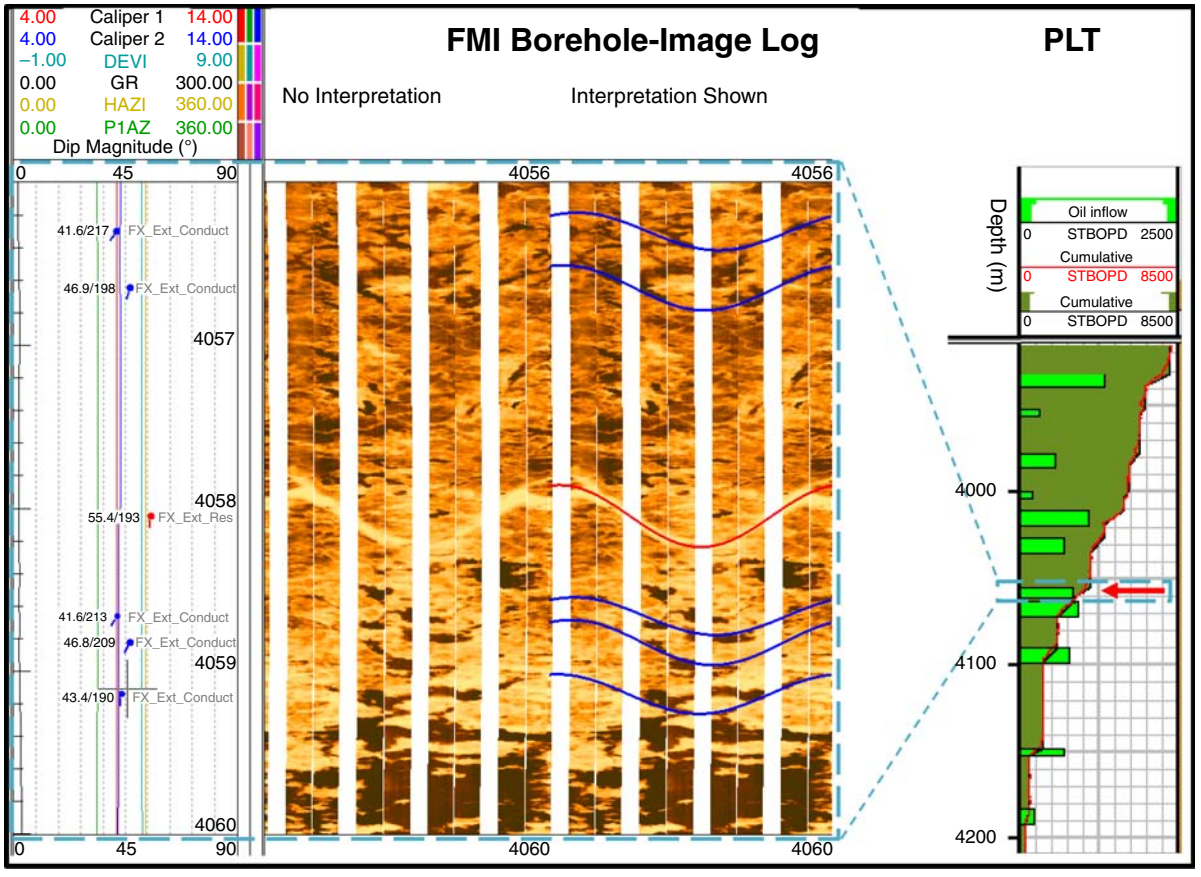

Fig. 8—From Well P-10, an example of an open, resistive (light-toned) fracture on the borehole-image log that is likely the source of oil flowing into the borehole, indicated in the PLT flowmeter interpretation (red arrow).

Discussions

The original methods to calculate permeability tensors proposed by Ramey (1975) and Kamal (1983) apply to single-medium homogeneous reservoirs. This method directly uses individual-interwell-test-analysis results. Even the analysis of each interwell set is not limited to any model; the derivation of the directional permeabilities at the location of the center well assumes the area around it is homogeneous. This idea of local homogeneity is similar to how single-well-test results are treated in a heterogeneous reservoir. It has become common practice in history matching that the formation properties in a well-drainage area in a numerical heterogeneous model are adjusted usually with a multiplier to honor buildup-test-analysis results (Pan et al. 2016; Levchenko et al. 2017). A similar strategy can be applied to modify the local anisotropy in the influence area of interwell tests in a heterogeneous model to honor the permeability tensors derived from our method. It is a regional approximation at the well-spacing scale to approach field heterogeneity. Nevertheless, it provides valuable information regarding the local anisotropy of real reservoirs.

Any modern techniques can be used to analyze each set of the interwell test. In the Korolev Field case, dual-porosity models are used to derive the fast-path properties, permeability k, porosity ϕ, storativity ω, and interporosity-flow coefficient λ. Compared with a single-porosity reservoir with the same permeability and porosity, the matrix/fracture properties ω and λ do affect the interference responses, but to a lesser degree than the dominant factor of the k/ϕ ratio. The smaller ω and/or λ are, the faster the response will be. In other words, the more hydrocarbons there are in the fracture network and/or the earlier interporosity flow from the matrix to the fracture occurs, the slower the response will be. In the proposed method to calculate directional permeabilities from individual-interwell-test-analysis results, only permeability and porosity are used. The effects of ω and λ are not considered. However, we have performed synthetic studies, and the results showed that the effects of these two parameters on production are secondary compared with effective formation permeability and well skin factor, especially in between well and global field scale. Hence, although the estimated permeability tensors in a dual-porosity system might carry certain errors, the method is nevertheless practical in providing reasonable values of directional permeabilities at the well-spacing scale, and the anisotropic ratio of $k_{\max}$ and $k_{\min}$ is reliable. In addition, the derived permeability tensors will eventually be used to adjust local anisotropy in numerical dual-porosity models.

Ultimately, all the information that can be derived from transient tests, such as formation properties and varying local directional permeabilities, can be used in numerical-simulation studies for discrete descriptions of anisotropic heterogeneous reservoirs.

Conclusions

1. A practical method of estimating directional permeabilities is developed to use well coordinates and the analysis results of individual interwell transient tests directly in heterogeneous reservoirs through mathematical matrix operations. This method has already been implemented in some commercial well-test-analysis software.
2. It is efficient and easy to use according to the way we collect transient data, which is dependent on project objectives, operation opportunities, and more data with time.
3. Each individual interwell test can be analyzed using any conventional or modern methods (type-curve match, analytical, semianalytical, or numerical models).
4. Comparing the fast-path properties derived from interwell-test analysis with the corresponding effective average values obtained from individual buildup tests at the wells could provide information regarding a highly conductive path (fracture network or channels) in the reservoir. If the formation properties from these two different types of tests are similar, it implies that the distribution of the highly conductive medium, if it exists, is relatively uniform. If the flow capacity of the fast path from the interwell test is much higher than the average value from the buildup test, it indicates there is a highly conductive path linking the wells.
5. The method of calculating directional permeabilities requires at least three sets of interference or pulse tests at different directions through the same well at each location. If more than three sets of interwell tests are available, we select the most-representative directions depending on reservoir structure, geological features, and those tests with high-quality data. The tests conducted at evenly separated arithmetic directions usually provide more-accurate solutions. If testing directions are clustered within a narrow angle, the solution is biased, or it might not converge to a solution.
6. With enough interwell transient data, a fieldwide permeability-tensor map can be easily generated. The information can be compared with that from geological information and static data. The permeability tensors from dynamic transient data are at the well-spacing scale. The static data are from wellbores and the scale is usually small, in inches. Integrating the interpretation results from both types of data reduces uncertainty in reservoir characterization.
7. The application of the proposed method in a large carbonate reservoir demonstrates its practicality even in fields with complex varying anisotropy.

Nomenclature

B = formation volume factor, RB/STB
c_t = total compressibility, psi^{-1}
dx, dy = relative coordinates, ft
h = net pay, ft
k = permeability, md
k^{eff} = effective permeability, md
$k_{\max}$ = maximum permeability, md
$k_{\min}$ = minimum permeability, md
L = individual fracture length, ft
$\boldsymbol{M}_{ij}$ = well coordinate matrix
$\boldsymbol{N}_{ij}$ = inverse matrix of well coordinate
p = pressure, psi
p_D = dimensionless pressure, dimensionless
q = flow rate, STB/D
q_0 = initial flow rate, STB/D
r = distance between wells, ft
r_D = dimensionless well distance, dimensionless
$\boldsymbol{R}_j$ = analysis results tensor
s = well skin factor, dimensionless

t = time, hours
t_D = dimensionless time, dimensionless
x, y = coordinates, ft
α = coefficient in matrix calculation
Δp = pressure change, psi
Δp_D = dimensionless pressure change, dimensionless
Δt = time lag, minutes
Δt_c = cycle time, minutes
Δt_{cD} = dimensionless cycle time, dimensionless
θ = angle with respect to x-directions
λ = interporosity flow coefficient
μ = viscosity, cp
ϕ = porosity, fraction
ω = fracture storativity ratio, dimensionless

Acknowledgments

The authors would like to thank Tengizchevroil and its partners Chevron, ExxonMobil, KazMunayGas, and Lukoil for the financial support and technical input for this work.

References

Abdrakhmanova, A., Iskakov, E., King, G. R. et al. 2014. Probabilistic History Matching of Dual-Porosity and Dual-Permeability Korolov Model Using Three Discrete Fracture Models. Presented at the SPE Annual Technical Conference and Exhibition, Amsterdam, 27–29 October. SPE-170854-MS. https://doi.org/10.2118/170854-MS.

Araujo, H. N., Andina, S. A., Gilman, J. R. et al. 1998, Analysis of Interference and Pulse Tests in Heterogeneous Naturally Fractured Reservoirs. Presented at the SPE Annual Technical Conference and Exhibition, New Orleans, 27–30 September. SPE-49234-MS. https://doi.org/10.2118/49234-MS.

Bachtel, S., Iskakov, E., Jenkins, S. et al. 2014. Seismic Facies and Geomorphology at Korolev Oil Field, Pricaspian Basin, Kazakhstan: Integration of Seismic, Image Log, and Core Leads to Improved Static Models. Oral presentation given at the AAPG Annual Convention and Exhibition, Houston, 6–9 April.

Collins, J., Narr, W., Harris, P. M. et al. 2013. Lithofacies, Depositional Environments, Burial Diagenesis, and Dynamic Field Behavior in a Carboniferous Slope Reservoir, Tengiz Field (Republic of Kazakhstan), and Comparison With Outcrop Analogs. In *Deposits, Architecture, and Controls on Carbonate Margin, Slope and Basinal Settings*, Vol. 105, ed. K. Verwer, T. E. Playton, and P. M. Harris, 50–83. Tulsa: Society for Sedimentary Geology.

Deruyck, B. G., Bourdet, D. P., DaPrat, G. et al. 1982. Interpretation of Interference Tests in Reservoirs with Double Porosity Behavior—Theory and Field Examples. Presented at the SPE Annual Technical Conference and Exhibition, New Orleans, 26–29 September. SPE-11025-MS. https://doi.org/10.2118/11025-MS.

Kamal, M. and Brigham, W. E. 1976. Design and Analysis of Pulse Tests With Unequal Pulse and Shut-In Periods. *J Pet Technol* **28** (2): 205–212. SPE-4889-PA. https://doi.org/10.2118/4889-PA.

Kamal, M. M. 1979. The Use of Pressure Transients to Describe Reservoir Heterogeneity. *J Pet Technol* **31** (8): 1060–1070. SPE-6885-PA. https://doi.org/10.2118/6885-PA.

Kamal, M. M. 1983. Interference and Pulse Testing—A Review. *J Pet Technol* **35** (12): 2257–2270. SPE-10042-PA. https://doi.org/10.2118/10042-PA.

Kamal, M. M. 2009. *Transient Well Testing*, Vol. 23. Richardson, Texas: Monograph Series, Society of Petroleum Engineers.

Kamal, M. M., Pan, Y., Landa, J. L. et al. 2005. Numerical Well Testing: A Method to Use Transient Testing Results in Reservoir Simulation. Presented at the SPE Annual Technical Conference and Exhibition, Dallas, 9–12 October. SPE-95905-MS. https://doi.org/10.2118/95905-MS.

Levchenko, P., Iskakov, E, Chalak, A. et al. 2017. Development of Fracture Models for Korolev Field: Characterization to Simulation. Presented at the SPE Annual Caspian Technical Conference and Exhibition, Baku, Azerbaijan, 1–3 November. SPE-189016-MS. https://doi.org/10.2118/189016-MS.

Narr, W., Schechter, D. S., and Thompson, L. B. 2006. *Naturally Fractured Reservoir Characterization*. Richardson, Texas: Society of Petroleum Engineers.

Pan, Y., Hui, M.-H., Narr, W. et al. 2016. Integration of Pressure Transient Data in Modeling Tengiz Field, Kazakhstan—A New Way to Characterize Fractured Reservoirs. SPE *Res Eval & Eng* **19** (1): 5–17. SPE-165322-PA. https://doi.org/10.2118/165322-PA.

Papadopulos, I. S. 1965. Nonsteady Flow to a Well in an Infinite Anisotropic Aquifer. Oral presentation given at the Symposium on Hydrology of Fractured Rocks, Dubrovnik, Yugoslavia, 7–14 October.

Ramey, H. J. Jr. 1975. Interference Analysis for Anisotropic Formations—A Case History (includes associated paper 6406). *J Pet Technol* **27** (10): 1290–1298. SPE-5319-PA. https://doi.org/10.2118/5319-PA.

Tankersley, T. H., Narr, W., King, G. R. et al. 2010. Reservoir Modeling to Characterize Dual Porosity, Tengiz Field, Republic of Kazakhstan. Presented at the SPE Caspian Carbonates Technology Conference, Atyrau, Kazakhstan, 8–10 November. SPE-139836-MS. https://doi.org/10.2118/139836-MS.

Yan Pan is the team leader of the Dynamic Reservoir Characterization Group with Chevron Energy Technology Company in Houston. Her experience includes well testing, production-data analysis, and data integration in Earth and reservoir models, as well as training Chevron engineers in these areas of technology. Pan holds a bachelor's degree in engineering mechanics from Tsinghua University, China, and master's and PhD degrees in petroleum engineering from Stanford University. The author of several SPE papers and publications, she served as the program chairperson for the SPE Golden Gate Section, the chairperson of the SPE Well Testing Technical Interest Group, and an SPE Distinguished Lecturer (2011–2012). Pan is a recipient of the Chevron Excellence in Reservoir Engineering Award, the SPE Western North America Regional Formation Evaluation Award, and the SPE Distinguished Technical Editor Award.

Medhat (Med) M. Kamal is a Chevron fellow emeritus, the chairperson of the SPE Golden Gate Section, and the general chairperson of the 2019 SPE Western Regional Meeting. He has more than 40 years of industry experience in well testing, reservoir description, and production and reservoir engineering. Kamal is the lead author and editor of SPE Monograph 23 *Transient Well Testing*, and has published more than 35 technical papers in various SPE journals. He holds a bachelor's degree from Cairo University and master's and PhD degrees from Stanford University, all in petroleum engineering. Kamal has been an SPE Distinguished Lecturer (1997–1998 and 2018–2019) and has won several regional and international awards, including the SPE Cedric K. Ferguson Gold Medal, the SPE Formation Evaluation Award, the SPE Distinguished Service Award, and the Texas Petroleum Engineer of the Year Award. He is an SPE Honorary Member. Kamal served as a member and as the chairperson of the SPE

Annual Technical Conference and Exhibition Well Testing, Textbook, and Monograph committees, and as a technical editor, review chairperson, and executive editor of *Journal of Petroleum Technology* and *SPE Reservoir Evaluation & Engineering*. He was the first chairperson of the SPE Board Committee on Research and Development and the chairperson of the first SPE conference on research and development. Kamal served on the SPE International Board of Directors (2007–2009) as the regional director of western North America.

Wayne Narr is an independent consultant. He recently retired from Chevron Energy Technology Company, where he was a senior research consultant. Narr is a structural geologist interested in the characterization and modeling of naturally fractured reservoirs. He has written research articles and an SPE book on naturally fractured reservoirs, and he has spoken on this topic as an SPE Distinguished Lecturer. Narr teaches courses on naturally fractured reservoirs and is currently creating online-based training and virtual field trips. He holds a PhD degree from Princeton University; a master's degree from the University of Toronto, Canada; and a bachelor's degree from Pennsylvania State University. Narr is a member of SPE.